Suppression of human prostate tumor growth by a unique prostate-specific monoclonal antibody F77 targeting a glycolipid marker

Geng Zhang[a], Hongtao Zhang[a], Qiang Wang[a], Priti Lal[a], Ann M. Carroll[a], Margarita de la Llera-Moya[b], Xiaowei Xu[a], and Mark I. Greene[a,1]

[a]Department of Pathology and Laboratory Medicine, University of Pennsylvania, Philadelphia, PA 19104-6082; and [b]Lipid Research Group, Children's Hospital of Philadelphia, Philadelphia, PA 19104-4318

Communicated by Peter C. Nowell, University of Pennsylvania School of Medicine, Philadelphia, PA, November 23, 2009 (received for review July 31, 2009)

In our effort to find diagnostic markers and to develop therapeutic approaches for prostate cancer, we have identified an mAb that is capable of binding to a cell surface antigen specifically expressed on both androgen-dependent and androgen-independent prostate cancer cells. Immunohistological studies revealed that this mAb, called F77, stained 112 of 116 primary and 29 of 34 metastatic human prostate cancer specimens. Although the mAb F77 alone directly promotes prostate cancer cell death, it also mediates complement-dependent cytotoxicity and antibody-dependent cellular cytotoxicity. In addition, mAb F77 can significantly inhibit androgen-independent PC3 and Du145 tumor growth in nude mice. Antigen characterization revealed that mAb F77 recognizes a very small molecular species with glycolipid properties. F77 antigen is concentrated in the lipid-raft microdomains, which serve as platforms for the assembly of associating protein complexes. Thus, the present study indicates that mAb F77 defines a unique prostate cancer marker and shows promising potential for diagnosis and treatment of prostate cancer, especially for androgen-independent metastatic prostate cancer.

androgen-independent tumor | antibody therapy | prostate cancer lipid antigen (PCLA) | antibody-dependent cellular toxicity | lipid rafts

Prostate cancer is the second leading cause of cancer-related death in men in the United States. Thirty percent to 45% of patients with clinically localized disease are found to have extracapsular extension (1), and cancer may relapse and metastasize after local therapy. Despite the effectiveness of hormone therapy, most patients with metastatic disease eventually progress to an androgen-independent state, at which time the disease is incurable. The 5-y survival rate for metastatic prostate cancer is only 34% (2). New therapeutic approaches are clearly needed for the treatment of advanced and metastatic prostate cancer.

Targeted monoclonal antibody therapy has proven efficacious in clinical cancer treatment. Certain mAbs, such as the anti-CD20 mAb (rituximab) used to treat B cell lymphoma and the anti-$p185^{Her2/neu}$ mAb (trastuzumab) for metastatic breast cancer, have been reasonably efficacious on their own (3, 4). Our laboratory showed that mAbs to $p185^{Her2/neu}$ can reverse the malignant phenotype and render tumors more susceptible to concomitant genotoxic therapies (5).

The antibodies currently available for detection and treatment of prostate cancers are limited. The mAb 7E11-C5.3, which binds to prostate-specific membrane antigen (PSMA), has been developed for clinical trials (6). The ProstaScint scan (Cytogen), based on ^{111}In-labeled 7E11-C5.3, appears superior to the conventional imaging methods for soft-tissue disease, but has limitations because it binds to the intracellular domain on PSMA (7). In addition, PSMA is not expressed in certain advanced, androgen-independent tumor cells such as PC3 and Du145, and therefore this antibody is not useful for imaging bone metastases. Recent studies show that the anti–prostate stem cell antigen (PSCA) mAb1G8 can inhibit tumor growth of androgen-dependent tumor xenografts (8). However, anti-PSCA mAbs are usually ineffective against androgen-independent tumors, which generally do not express PSCA (9). An analysis of prostate cancer tissue sections demonstrated that PSCA is absent in approximately 20% of specimens (10). Therefore, defining new prostate-specific markers is important to improve the diagnosis and treatment of advanced androgen-independent prostate cancer.

A large percentage of androgen-independent prostatic carcinomas metastasize to bone. These metastases are difficult to treat and contribute to increased morbidity and mortality. The PC3 cell line was originally derived from advanced androgen-independent bone metastasis and has become a commonly used cell model for studying androgen-independent prostate cancer. We immunized mice with PC3 cells and produced mAb F77 (11). The present study shows that mAb F77 recognizes a unique glycolipid antigen highly restricted to the prostate cancer cell surface. We term the antigen prostate cancer lipid antigen (PCLA). The unique binding pattern of mAb F77 indicates that PCLA exists predominantly in prostate and that its expression is consistently higher in tumor tissues than in normal tissues. Because PCLA remains expressed on both androgen-dependent and androgen-independent prostate cancer, it may be exploited as a target for diagnosis and treatment of both early and late stages of the disease.

Results

mAb F77 Specifically Recognizes Prostate Cancer Cells and Tissues. Flow cytometry analysis of the murine IgG3 mAb F77 binding reveals that its targeting antigen is expressed at a high level on androgen-independent prostate cancer cell surfaces (e.g., PC3-MM2, PC3, and Du145) and at a slightly lower level on the androgen-dependent LNCaP cell surfaces (Fig. 1). mAb F77 shows very limited binding to certain cell lines of mammary or ovarian origin but fails to bind to any cell lines from lung, kidney, or skin (Table S1). SW260 colon cancer cells and BxPC3 pancreatic cancer cells can also be weakly stained by mAb F77.

mAb F77–based immunohistochemistry was performed on a wide range of normal and cancerous prostate tissues. mAb F77 staining was significantly more intense in prostate cancerous tissues than in benign prostate tissues, in which mAb F77 showed only focal staining on a subpopulation of prostate glandular cells (Fig. 2*A*). Using primary prostate cancer tissue microarrays, we found that 112 of 116 prostate tissue cores (96.6%) were positive for F77 staining (Fig. 2*B*). The four negative cases were well differentiated prostate carcinomas. Some minimal staining was

Author contributions: G.Z. and M.I.G. designed research; G.Z., P.L., A.M.C., M.d.l.L.-M., and X.X. performed research; G.Z., H.Z., Q.W., and M.I.G. analyzed data; and G.Z., H.Z., Q.W., and M.I.G. wrote the paper.

The authors declare no conflict of interest.

[1]To whom correspondence should be addressed. E-mail: greene@reo.med.upenn.edu.

This article contains supporting information online at www.pnas.org/cgi/content/full/0911397107/DCSupplemental.

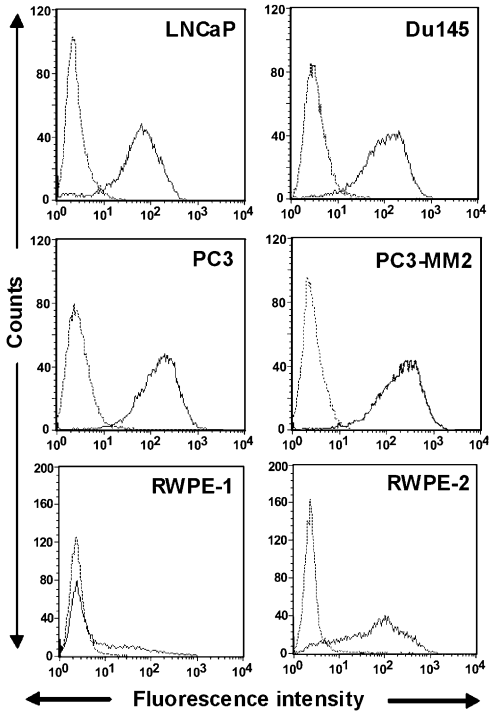

Fig. 1. Binding of mAb F77 to prostate cancer cell lines. Androgen-dependent LNCaP and androgen-independent Du145 and PC3 are commonly used prostate cell lines. PC3-MM2 is a highly metastatic PC3-derived cell line. RWPE-1 is a normal human prostate epithelial cell line immortalized by HPV-18. Tumorigenic prostate epithelial cell line RWPE-2 was derived from RWPE-1 with *K-ras* oncogene transfection. mAb F77 is represented by the bold line and irrelevant mouse IgG3 by the dashed line.

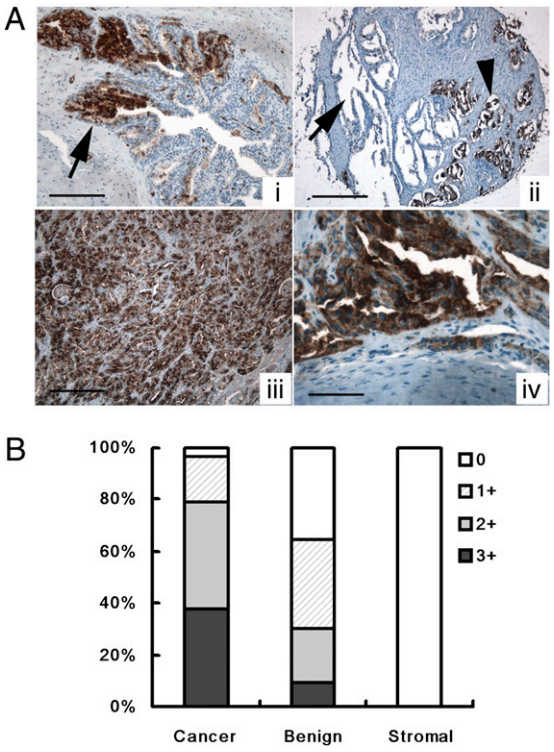

Fig. 2. Binding of mAb F77 to prostate tissue samples. (*A*) mAb F77 immunohistochemical staining in prostate tissue. In benign prostate glands (*i*) there is a mosaic staining pattern of some benign prostate glands. Arrow points to the F77-positive prostate gland. (Scale bar, 100 μm.) Benign prostate glands are negative for mAb F77 (arrow, *ii*), whereas cancerous prostate glands are positive (arrowhead, *ii*). (Scale bar, 200 μm.) In high-grade prostate cancers (*iii*) poorly differentiated prostate cancerous tissues are diffusely positive for mAb F77. (Scale bar, 50 μm.) In bone metastasis (*iv*) cancerous glands in a bone metastasis are also diffusely positive. (Scale bar, 25 μm.) (*B*) Quantification of Immunohistochemical staining of mAb F77. Specimens ($n = 116$) were stained with mAb F77 (1 μg/mL). Staining intensity of the tissues was graded as 0 (negative), 1+ (weak), 2+ (moderate), and 3+ (strong).

observed in a small fraction of small blood vessels in human brain. In addition, 29 of 34 prostate metastatic specimens (85.3%) were positive for F77. No specific staining was found in normal or tumor tissues of human colon, kidney, cervix, pancreas, lung, skin, and bladder (Table S1). These results indicate that the F77 antigen is highly restricted to prostate and overexpressed in prostate tumors.

F77-Positive Subpopulation of RWPE-1 Cells Displays Tumorigenic Phenotypes. mAb F77 binds to a small population (<10%) of the nontumorigenic human prostate epithelial cell line RWPE-1, but binds with greater intensity to >80% of tumorigenic RWPE-2 cells that were derived from RWPE-1 after transfection with the constitutively active *K-ras* oncogene (Fig. 1). RWPE-2 cells that express the F77 antigen grow faster and display enhanced colony-forming activity compared with F77-negative RWPE-1 cells (12). Most importantly, the parent RWPE-1 cells do not form tumors when injected into nude mice, whereas RWPE-2 cells do. The F77 antigen may be used as a cell surface biomarker indicating malignant transformation of prostate cells such as RWPE-1.

To address whether F77 antigen expression is associated with the tumorigenic phenotype of prostate epithelial cells, RWPE-1 cells were stained with mAb F77 and sorted into F77-positive and F77-negative subpopulations by FACS. After 7 d of in vitro cell culture, $F77^+$/RWPE-1 maintained a high level of F77 antigen expression on cell surfaces with a comparable staining pattern to RWPE-2. The growth of $F77^+$/RWPE-1 was twice as fast as that of $F77^-$/RWPE-1 (Fig. S1).

Next, we compared the ability of the $F77^-$ and $F77^+$ subpopulations derived from RWPE-1 to initiate tumors in nude mice (Table S2). Immediately after cell sorting, cells were mixed at a 1:1 dilution with Matrigel (BD Biosciences) and injected into nude mice (0.5×10^6 cells per mouse). As a positive control for tumor formation, tumorigenic RWPE-2 cells were also injected. Significantly, injection of $F77^+$/RWPE-1 cells resulted in tumors in four of six mice, the same ratio as tumorigenic RWPE-2 cells, whereas $F77^-$/RWPE-1 cells resulted in a single tumor (one of six). These results demonstrate that F77-positive RWPE-1 cells display increased tumorigenic properties compared with F77-negative prostate epithelial cells.

Effects of mAb F77 on Prostate Cancer Cells. PC3 cells exposed to mAb F77 for 4 h were counterstained with Annexin V and propidium iodide (Fig. 3*A*). Cells stained with Annexin V alone represent cells at an early stage of apoptosis, whereas cells stained with both Annexin V and propidium iodide are considered to exist in a more advanced stage of apoptosis/necrosis. PC3 cells exposed to 3 μg/mL mAb F77 displayed 4% staining with Annexin V alone and 8% staining with Annexin V and propidium iodide, indicating that interaction of mAb F77 with its cognate antigen on cells predisposes the cells to modest levels of apoptosis. Fewer than 1% of PC3 cells exposed to control murine IgG3 displayed staining with Annexin V alone, and there was no difference between mAb F77 and control IgG3 on control cell line A431.

Mouse IgG3 antibodies can mediate both complement-dependent cytotoxicity (CDC) and antibody-dependent cellular cytotoxicity (ADCC) (13). mAb F77-induced CDC was evaluated by MTT assays. Fig. 3*B* shows that the presence of 1% of either

CELL BIOLOGY

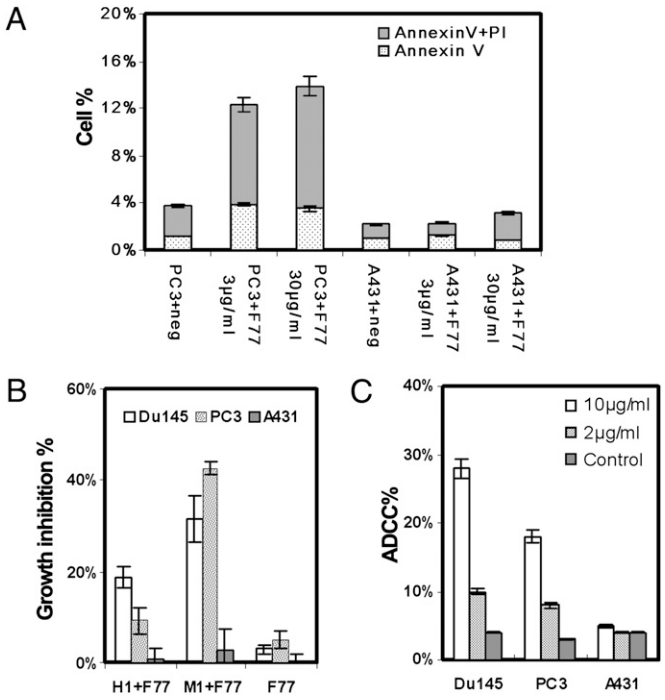

Fig. 3. Effects of mAb F77 on prostate cancer cells in vitro. (*A*) Apoptosis assay by Annexin V and propidium iodide staining. Bars indicate percentages of cells stained with Annexin V and propidium iodide. A431 and PC3 cells were treated with 3 or 30 μg/mL mAb F77 for 4 h at 37°C. (*B*) MTT assay with 25 μg/mL mAb F77 in 100 μL medium containing 1% human serum (*H1+F77*) and 25 μg/mL mAb F77 in 100 μL medium containing 1% mouse serum (*M1+F77*). Cell viability was measured by standard MTT assay. *Growth inhibition %*, [(control wells – treated wells) / control wells] × 100. Growth inhibition percentage increased in response to the addition of either mouse or human serum, indicating mAb F77 induced CDC. (*C*) ADCC assay: PC3 or Du145 target cells were treated with different concentrations of mAb F77 (0, 2, and 10 μg/mL) at an effector-to-target cell ratio of 2:1. A431 cells were used as control cells. ADCC percentage calculation followed the instruction from a CytoTox 96 nonradioactive cytotoxicity assay (Promega). Negative controls are cells treated with an irrelevant murine IgG3 mAb. Data are expressed as mean ± SD of triplicate measurements.

mouse or human serum as a source of complement remarkably decreased the number of viable cells. We noted a 32% reduction of viable Du145 cells and 43% reduction of PC3 cells when treated with 25 μg/mL mAb F77 in 1% mouse serum. mAb F77, alone in the absence of complement, for example when tested on cells growing in serum-free medium or in heat-inactivated serum, caused a limited decrease of cell viability (approximately 4%).

ADCC of F77 against prostate tumor cells was examined in vitro by lactate dehydrogenase release assay. Monocyte-like U937 cells with IFN-γ treatment were used as effector cells (14). Fig. 3*C* presents a significant increase of cytolysis by 10 μg/mL mAb F77 at an effector-to-target cell ratio of 2:1, revealing 28% cytotoxicity of Du145 and 18% of PC3 cells. The mAb F77 ADCC effect was antigen-specific, as A431 cells, which lack the F77 antigen, were not affected.

mAb F77 Inhibits Growth of Prostate Tumors In Vivo. To determine if the effects of mAb F77 could be translated to inhibition of androgen-independent prostate tumor growth in vivo, the antibody was given to mice transplanted with PC3 or Du145 tumor cells. In the first series of experiments, nude mice were injected with PC3 cells (10^6 per mouse) on the right flank and A431 cells (0.5×10^6 per mouse) on the left flank. Antibody injection (i.p.) started when tumors were first palpable (2–4 mm^3) at day 7 after injection of tumor cells. mAb F77 was administered four times (200 μg/dose at days 7 and 9 and 100 μg/dose at days 11 and 13). A mouse IgG control (200 μg/dose) or vehicle (PBS solution) was also used.

Treatment with mAb F77 inhibited PC3 tumor growth. PC3 tumor growth was completely suppressed in five of six mice in the mAb F77 treatment group. The one exception did develop a small but palpable tumor (volume of 6 mm^3). Mice ($n = 6$) in the vehicle control group all developed tumors with an average volume of 173.9 mm^3 at day 28 (Fig. 4*A*). A431 tumors were not affected by F77 treatment and grew aggressively, with a mean size of 1,200 mm^3 by day 28 when they had to be killed (Fig. 4*B*).

Inhibition of tumor formation was also observed on Du145 tumors treated with mAb F77. Du145 group I was treated according to the same protocol as the PC3 group described earlier. Administration of mAb F77 to Du145-injected mice resulted in complete inhibition of tumor growth until day 30 compared with control mice treated with mouse IgG control (Fig. 4*C*).

In Du145 group II, we studied the effectiveness of mAb F77 on larger established tumors. D145 cells (2×10^6) were injected in each mouse in this group ($n = 6$). mAb F77 (200 μg/dose) was administrated every other day for a total of four injections, starting at day 11 when the mean size of the Du145 tumor was more than 30mm^3. A significant reduction ($P < 0.01$) in tumor growth rate was detected in mAb F77-treated mice compared with control mice (Fig. 4*D*). At day 28, 10 d after the last antibody injection, tumors in the mAb F77–treated mice reached a mean volume of 79.7 mm^3, whereas the control mice developed tumors with a mean volume of 195.8 mm^3. The F77 antibody is able to inhibit androgen-independent prostate tumor formation in both the PC3 and Du145 established tumor models.

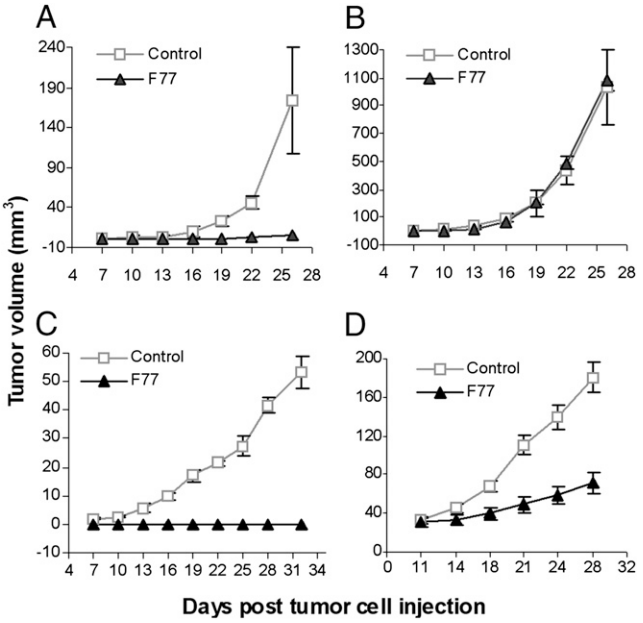

Fig. 4. Inhibition of androgen-independent prostate tumor growth by mAb F77. Male nude mice were injected s.c. with 1×10^6 PC3 on the right flank (*A*) and 0.5×10^6 A431 on the left flank (*B*). Treatment started at day 7 after tumor cell injection. mAb F77 was administered by i.p. injection of 200 μg per dose at days 7 and 9 and 100 μg per dose at day 11 and 13. PBS solution was used as the vehicle control. Mice have to be killed when tumors are greater than 1 cm in diameter in accordance with the University of Pennsylvania Institutional Animal Care and Use Committee. Du145 1×10^6 (*C*) and 2×10^6 (*D*) were transplanted onto male nude mice. mAb F77 or a control mouse IgG was administered at day 7 by i.p. injection of 200 μg per dose every other day for four times in total (*C*). Post-treatment (*D*) started at day 11 when tumor volume was greater than 30 mm^3. The data are presented as mean tumor volume (in mm^3) ± SEM; $P \leq 0.01$.

Characterization of the F77 Antigen. Characterization of the F77 antigen by conventional protein SDS/PAGE was unsuccessful. The F77 antibody was also not useful for Western blotting. After immunoprecipitation with mAb F77, samples were separated by SDS/PAGE (4–16%). A significant band that migrated even faster than the dye front (approximately <5 kDa) was detected in the PC3 sample by carbohydrate staining (Pro-Q Emerald 300 Gel Stain Kit; Invitrogen), but was not stained by Coomassie blue (Fig. 5*A*). Pro-Q Emerald 300 staining is based on the principle of periodic acid–Schiff staining as a way to detect carbohydrate chains in glycoproteins or glycolipids (15).

To identify the nature of the antigen recognized by mAb F77, PPMP (1-phenyl-2-palmitoylamino-3-morpholino-1-propanol), a potent inhibitor of glycosphingolipid synthesis, was added to cell cultures at concentrations of 5 or 20 μg/mL for 72 h. To prevent glycosylation of glycoproteins, the cells were cultured for 48 to 72 h with 2 to 4 mM O-glycosylation inhibitor benzyl-N-acetyl-α-galactosaminide (benzyl-α-GalNAc; B4894; Sigma) or 0.5 to 2 μg/mL N-glycosylation inhibitor Tunicamycin (Sigma) (16).

PPMP caused a significant dose-dependent decrease of F77 antigen on both PC3 and Du145 cell surfaces but had no effect on glycoprotein CD147 (Fig. 5*B*). The modest increase of CD147 level was caused by a decrease in cell viability after PPMP treatment. Two widely used inhibitors of protein glycosylation, Tunicamycin and benzyl-α-GalNAc, had no effect on F77 antigen expression (Fig. S2).

Moreover, glycolipid extracts by chloroform/methanol/water (1:2:1.4) of different cell lines were analyzed by lipid ELISA. mAb F77 displayed specific binding to the glycolipid extracts from PC3 and Du145 in a concentration-dependent manner, but binding to extracts of control human A431 and HEK293 cells was not observed (Fig. 5*C*).

Recent studies have revealed that glycolipids in cell membranes are preferentially distributed into lipid microdomains, also termed lipid rafts (17). We examined whether the glycolipid antigen of mAb F77 was also located in lipid rafts on the cell surface. Lipid rafts can be isolated biochemically as detergent-insoluble fractions when cells are treated with Triton X-100 or CHAPS on ice. 0.5% CHAPS lysis buffer was used to treat prostate cancer cells after the surfaces were saturated with F77 antibody (approximately 8 μg/10^7cells). As mAb F77 was already prebound to the antigen to form antibody–antigen complexes before detergent treatment, protein G beads were used to capture the soluble antibody–antigen complexes from the supernatant. The amount of F77 antibody was used as an indicator of detergent-soluble cognate antigens (Fig. S3). Using this detection system, only 4% of F77 antigens were soluble in 0.5% CHAPS (Fig. S3), suggesting F77 antigens exist in the detergent-insoluble fractions (namely lipid rafts). RIPA buffer treatment that can disrupt lipid rafts released a large percentage of F77 antigens from PC3 (70%) and Du145 (60%) cell membranes.

Taken together, these studies indicate that the F77 antigen is a prostate-specific glycolipid located in lipid raft microdomains on prostate cancer cell surfaces.

Discussion

The mAb F77 was produced after immunization of mice with the androgen-independent prostate cancer cell line PC3 (11). mAb F77 recognizes both androgen-independent and androgen-dependent prostate cancer cells (Fig. 1). mAb F77 displays a preferential reactivity with prostate cancer versus normal prostate tissues. Immunohistological studies have demonstrated that F77 staining intensity correlates with tumor grade (Fig. 2). Additionally, *K-ras* transfection up-regulates F77 antigen levels, and elevated expression of F77 antigen correlates with increased tumorigenic properties of prostate epithelial cells (Table S2).

Although mAb F77 alone modestly initiated direct cell death of prostate cancer cells as measured by Annexin V and PI assays,

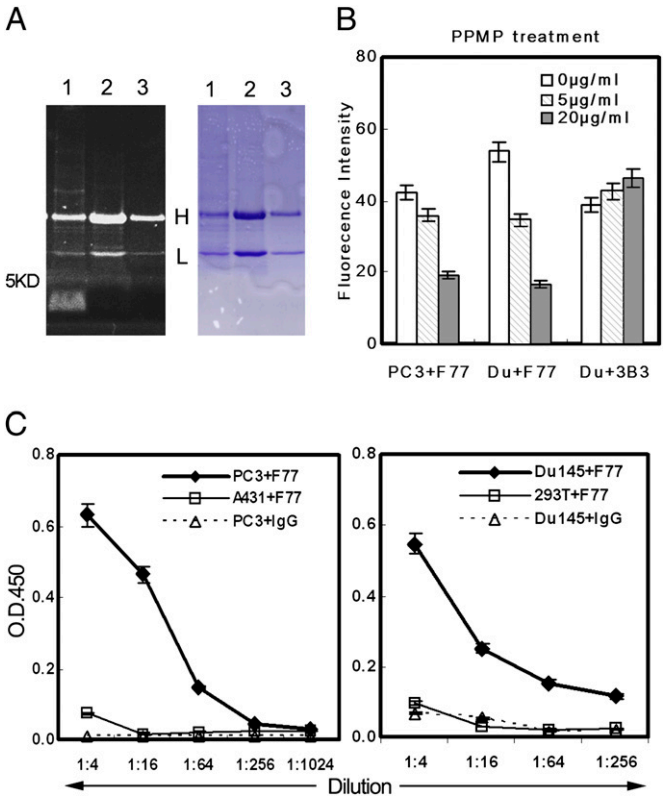

Fig. 5. Characterization of the F77 antigen. (*A*) F77 Immunoprecipitation. In lane 1, 1×10^7 PC3 cells bound with F77 antibody (10 μg) were treated with 1 mL RIPA buffer at 4°C for 30 min. After centrifugation at 10,000 × *g* for 1 h, supernatant was incubated with protein G beads at 4°C for 1 h. In lane 2, A431 cell lysate (10^7 cells/1 mL RIPA buffer) was immunoprecipitated with 10 μg mAb F77. In lane 3, PC3 cell lysate (10^7 cells/1 mL RIPA buffer) was immunoprecipitated with 5 μg mouse IgG. Samples were separated by Tris SDS/PAGE (4–16%). Gel was first stained with Pro-Q Emerald 300 carbohydrate staining (*Left*) following the instructions of the manufacturer, and then stained with Coomassie blue (*Right*). The fluorescent signal obtained with the Pro-Q Emerald 300 stain was visualized using a 300-nm transilluminator. (*B*) PPMP treatment of PC3 and Du145. After treating PC3 or Du145 cells with glycosphingolipid inhibitor PPMP (0, 5, or 20 μg/mL) for 48 h, the binding of mAb F77 to cells was analyzed by flow cytometry. PPMP treatment induced a dose-dependent decrease of the F77 antigen level on both PC3 and Du145 cell surfaces. (*C*) Specific binding of mAb F77 to glycolipid extracted from PC3 and Du145. Glycolipid extractions by chloroform/methanol from prostate cell lines PC3 and Du145 or control cell lines HEK293 and A431 were coated onto 96-well flat-bottom plates at a serial dilution (1:4–1:1,024) for ELISA with F77 antibody (1 μg/mL). Anti-CD147 monoclonal antibody 3B3 was used as a control murine IgG3.

CDC and ADCC are also important to the antitumor activity of mAb F77 in vitro and likely in vivo (Fig. 3). In the present study, mAb F77 effectively prevented tumor outgrowth in mice bearing PC3 and Du145 tumor xenografts (Fig. 4). As radiolabeled mAb F77 can specifically target small PC3 tumor xenografts in nude mice (18), treatment with radiolabeled F77 represents a plausible strategy for both primary and metastatic prostate cancer.

F77 antigen can be distinguished from other prostate tumor markers, such as PSMA, PSCA, and 6-transmembrane epithelial antigen of prostate protein (19), by its expression pattern on androgen-independent prostate cancer cell lines and the highly specific expression pattern on prostate cancerous cells and tissues.

We have demonstrated the glycolipid origin of the F77 antigen. No significant protein band has been detected to date in conventional SDS/PAGE analyses by Coomassie blue or silver staining from immunoprecipitation assays by mAb F77. Periodic acid–Schiff

carbohydrate staining revealed that this F77 antigen has a high degree of glycosylation and a low molecular weight (less than 5 kDa). An ELISA-based analysis of lipid extractions indicates that F77 antigen possesses glycolipid features in organic solvent extracts (Fig. 5). The existence of a small peptide component in F77 antigen remains to be determined in the future.

Although our studies have not determined the fine molecular structure of the F77 glycolipid antigen, we did find that antibody recognition was diminished by blocking glycolipid synthesis with PPMP. PPMP inhibits the synthesis of most glycosphingolipids by blockade of the enzyme glucosylceramide synthase (20). Glycosphingolipids are the most common glycolipids in mammals (21). Our data indicate that mAb F77 recognizes a unique prostate-specific glycolipid, termed PCLA.

Other monoclonal antibodies selected by preferential or specific reactivity with human cancer have been characterized as specific for glycolipids (22, 23). Some have been used in trials of antibody therapy for melanoma, colon cancer, and other cancers (24–26). Studies indicate that these glycolipid antigens are effective for complement lysis because of the short distance between the site of complement activation and the cell membrane (27–29). Our findings indicate that PCLA is also a target for antibody-mediated complement lysis.

The resistance of PCLA to detergent treatment reflects its distribution in biochemically defined lipid rafts on the cell membrane (Fig. S3). Glycolipids usually concentrate into lipid raft microdomains (21, 30), in which glycolipid can reach high local concentrations and provide the multivalent attachment for C1q binding to the antibody-coated cell surface, which might also contribute to the effectiveness of glycolipids as antitumor targets (31).

Lipid rafts mediate endocytosis of various plasma membrane molecules, including signaling receptors and glycosphingolipids, which are mainly found in lipid rafts (32, 33). Lipid raft endocytosis explains the internalization of PCLA upon F77 antibody binding (11). The remarkable efficiency of mAb F77-PCLA internalization may facilitate the use of mAb F77 in tumor-specific delivery of therapeutic molecules useful for prostate cancer treatment.

Extensive MS studies with coimmunoprecipitation by F77 antibody revealed that CD13, CD44, Na^+/K^+ ATPase, and cytoskeleton proteins are associated with PCLA enriched microdomains (Table S3). These findings are consistent with other studies showing the localization of CD13, CD44, and Na^+/K^+ ATPase in lipid rafts and the interaction between lipid rafts and the cytoskeleton (34–37).

Moreover, CD13 has been identified in prostasomes from both human semen samples and prostate cell culture medium (38, 39). PCLA was also detected on prostasomes isolated from PC3 medium by a sandwich ELISA and flow cytometry employing the F77 antibody (Fig. S4). Further clinical samples should be used to clarify the role of PCLA in prostasomes and whether PCLA is detectable in serum or semen samples.

Although the fine glycolipid structure of PCLA remains to be resolved, this prostate-specific glycolipid represents an attractive target for prostate cancer diagnosis and therapy.

Materials and Methods

For additional details, see *SI Methods*.

Cell Lines. PC3, Du145, LNCaP, RWPE-1, and RWPE-2 cells were obtained from the American Type Culture Collection. PC3-MM2 was purchased from Isaiah J. Fidler at the University of Texas M. D. Anderson Cancer Center. RWPE-1, a nontumorigenic human prostatic epithelial cell line, was developed by immortalization of epithelial cells derived from the peripheral zone of a normal human prostate (12). The RWPE-2 human prostatic carcinoma cell line was derived from RWPE-1 by transformation with *K-ras*. The base medium for RWPE-1 and RWPE-2 cells is provided by Invitrogen as Keratinocyte Serum Free Medium (K-SFM; Gibco). This kit is supplied with the two additives required to grow this cell line: bovine pituitary extract and human recombinant EGF. The other cell lines are maintained in RPMI medium (Invitrogen) containing 5% FBS (HyClone).

Immunohistochemistry Staining. All cases were retrieved from the surgical pathology files at the University of Pennsylvania Medical Center. F77 immunohistochemical staining was performed on 5-mm paraffin-embedded tissues including tissue microarray sections. Briefly, sections were deparaffinized in xylene and rehydrated in graded alcohols. A heat-based antigen retrieval method was used in citrate buffer (pH 6.0) in a microwave oven. F77 antibody (5 μg/mL diluted in antibody diluent; Dako) was added and incubated for 30 min at room temperature. Slides were washed five times with Tris-buffered saline solution containing Tween 20 (pH 7.6; Dako) and incubated for 30 min at room temperature with horseradish peroxidase–labeled dextran polymer coupled to antimouse (EnVision System HRP; Dako). Slides were then washed three times with Tris-buffered saline solution containing Tween 20, developed with diaminobenzidine, and counterstained with hematoxylin. The negative control lacked the primary antibody. Immunohistochemical stains for F77 were interpreted semiquantitatively by assessing the intensity of staining on the entire tissue sections or tissue microarray cores. The staining was read by two board-certified pathologists (P.L. and X.X.).

Flow Cytometry Assay. Cells ($0.5–1 \times 10^6$) were resuspended in 100 μL FACS buffer (1% BSA/PBS solution) containing 1 μg mAb F77 and incubated on ice for 20 min. After being washed twice with FACS buffer, cells were incubated with FITC-labeled goat antimouse antibody (1:100; Jackson ImmunoResearch) for 30 min on ice before analysis on a FACSCalibur system (BD Biosciences) using CellQuest Pro software. Cell sorting was carried out on FACSVantage SE with FACSDiVa Option-DiVa software in the Flow Cytometry and Cell Sorting Resource Laboratory at Penn Medicine Path BioResource.

MTT Assay. Prostate cell lines PC3 and Du145 were divided into aliquots (1,000 cells/well) into 96-well flat-bottom plates. The next day, the cells were treated with 1, 5, and 25 μg/mL mAb F77 or a murine IgG3 (negative control) in the presence of 1% or 10% mouse serum or human serum. Cells were incubated for 3 d at 37°C before the addition of 3-(4,5-dimethyl-2-thiazolyl)-2,5-diphenyl-2H-tetrazolium bromide (MTT) to each well, and absorbance was determined at 570 nm (40).

Cell Apoptosis Assay (Annexin V and Propidium Iodide). Tumor cells were detached by trypsin/EDTA and then washed twice with RPMI medium. Cells were exposed to 3 or 30 μg/mL mAb F77 or appropriate controls in RPMI medium for 2 to 6 h at 37°C in a humidified incubator, 5% CO_2. The cells (1×10^5) were then washed with cold PBS solution, stained for 15 min at room temperature in the dark with 5 μL Alexa 488–Annexin V and 1 μL propidium iodide (Vybrant Apoptosis Assay Kit 2; V13241; Invitrogen), and analyzed by dual color-flow cytometry.

ADCC Assay. Cytotoxic activity was assessed by using the CytoTox 96 nonradioactive cytotoxicity assay (Promega). Effector U937 cells were treated with IFN-γ (100 U/mL) for 12 to 24 h and then washed three times with serum-free medium and incubated for 2 h to allow detachment of IgG possibly absorbed from bovine serum (14). Prostate cancer cell lines PC3 and Du145 were target cells, whereas A431 was the control cell line. For ADCC assays, mAb F77 was incubated with target cells (10^4 per well) for 20 min before addition of effector cells. After 8 to 16 h incubation at 37°C, 50 μL supernatant was removed from each well, transferred to an enzymatic assay plate, mixed with 50 μL reconstituted substrate mix, and incubated for 30 min at room temperature (protected from light). Stop solution (50 μL) was added to each well and absorbance at 490 nm was recorded. Each test was performed in triplicate. The results are expressed as the percentage of lysis (ADCC%).

Xenograft Mouse Models. Tumor xenografts were generated by s.c. injection of 0.5×10^6 A431 or 1 to 2×10^6 PC3 or Du145 cells with or without Matrigel (BD Biosciences) in the flanks of male NCr athymic-nu/nu mice (Charles River Laboratory). Intraperitoneal antibody injection started at day 7 or 11 after tumor cell implantation. Control mice were injected with irrelevant mouse IgG or PBS solution, which had no effect on tumor growth. Tumor size was determined by vernier caliper measurements, and the tumor volume was calculated (in mm^3) as length × width × height.

Extraction of F77 Antigen by Chloroform/Methanol. A 2×10^8 cell pellet was homogenized with three volumes of distilled water. The homogenate was poured into 10.8 volumes of methanol at room temperature and then 5.4 volumes of chloroform were added. The mixture was stirred for 30 min and was then filtered; 3.5 volumes of water were then added. The solvents were carefully mixed by turning the glass tube up and down several times. When the two

phases were distinctly separated, the upper phase was collected and evaporated to dryness. The residue was resuspended in water or methanol for the subsequent analysis (41).

Lipid ELISA for F77 Antigen. Fourfold dilution of the antigen samples was made in methanol. Immediately before addition to microplate wells, sample dilutions were mixed well with an equal volume of water. A 50-μL aliquot was then pipetted into each well of a 96-well flat-bottom plate. The solvent was allowed to evaporate at room temperate for 12 h. The plates were blocked by 1% BSA/PBS solution for 2 h at room temperature. After three washes with PBS solution, F77 antibody or control mouse antibody was diluted with PBS solution, and 50 μL was added to each well. After 90 min of incubation, the plates were washed three times with PBS solution. Secondary antibody (1:5,000 diluted HRP–goat anti-mouse; GE Healthcare) was then added and the plates were incubated for 1 h at room temperature. The plates were washed five times; the color was developed with 3,3,5,5-tetramethylbenzidine (Sigma) and measured at 450 nm (42).

Statistical Analysis. All experiments were repeated three times. The data are expressed as means ± SD. Statistical analysis was performed using Student *t* test. The criterion for statistical significance used was $P < 0.05$.

ACKNOWLEDGMENTS. This work was partially supported by funding from the Jay Sigel Invitational Golf Event, the National Cancer Institute (M.I.G.), and a grant from Nidus Therapeutics to H.Z. and Q.W. M.I.G. is the John Eckman Professor of Medical Science at University of Pennylvania. We thank G.H. Rothblat for discussion and advice. We also thank Penn Proteomics Core Facility for mass spectrometry services.

1. Sandblom G, Dufmats M, Nordenskjöld K, Varenhorst E; South-East Region Prostate Cancer Group (2000) Prostate carcinoma trends in three counties in Sweden 1987-1996: results from a population-based national cancer register. *Cancer* 88:1445–1453.
2. Noldus J, et al. (2000) Stage migration in clinically localized prostate cancer. *Eur Urol* 38:74–78.
3. Maloney DG, et al. (1997) IDEC-C2B8 (Rituximab) anti-CD20 monoclonal antibody therapy in patients with relapsed low-grade non-Hodgkin's lymphoma. *Blood* 90: 2188–2195.
4. Drebin JA, Link VC, Stern DF, Weinberg RA, Greene MI (1985) Down-modulation of an oncogene protein product and reversion of the transformed phenotype by monoclonal antibodies. *Cell* 41:697–706.
5. O'Rourke DM, et al. (1998) Inhibition of a naturally occurring EGFR oncoprotein by the p185neu ectodomain: implications for subdomain contributions to receptor assembly. *Oncogene* 16:1197–1207.
6. Bander NH, et al. (2005) Phase I trial of 177lutetium-labeled J591, a monoclonal antibody to prostate-specific membrane antigen, in patients with androgen-independent prostate cancer. *J Clin Oncol* 23:4591–4601.
7. Morris MJ, et al. (2005) Pilot trial of unlabeled and indium-111-labeled anti-prostate-specific membrane antigen antibody J591 for castrate metastatic prostate cancer. *Clin Cancer Res* 11:7454–7461.
8. Reiter RE, et al. (1998) Prostate stem cell antigen: a cell surface marker overexpressed in prostate cancer. *Proc Natl Acad Sci USA* 95:1735–1740.
9. Saffran DC, et al. (2001) Anti-PSCA mAbs inhibit tumor growth and metastasis formation and prolong the survival of mice bearing human prostate cancer xenografts. *Proc Natl Acad Sci USA* 98:2658–2663.
10. Wente MN, et al. (2005) Prostate stem cell antigen is a putative target for immunotherapy in pancreatic cancer. *Pancreas* 31:119–125.
11. Carroll AM, et al. (1984) Monoclonal antibodies to tissue-specific cell surface antigens. I. Characterization of an antibody to a prostate tissue antigen. *Clin Immunol Immunopathol* 33:268–281.
12. Webber MM, Bello D, Quader S (1997) Immortalized and tumorigenic adult human prostatic epithelial cell lines: characteristics and applications Part 2. Tumorigenic cell lines. *Prostate* 30:58–64.
13. Carter PJ (2006) Potent antibody therapeutics by design. *Nat Rev Immunol* 6:343–357.
14. Akiyama Y, Lubeck MD, Steplewski Z, Koprowski H (1984) Induction of mouse IgG2a- and IgG3-dependent cellular cytotoxicity in human monocytic cells (U937) by immune interferon. *Cancer Res* 44:5127–5131.
15. Tatituri RV, et al. (2007) Inactivation of Corynebacterium glutamicum NCgl0452 and the role of MgtA in the biosynthesis of a novel mannosylated glycolipid involved in lipomannan biosynthesis. *J Biol Chem* 282:4561–4572.
16. Paul P, Bordmann A, Rosenfelder G, Towbin H (1992) Simultaneous determination of sugar incorporation into glycosphingolipids and glycoproteins. *Anal Biochem* 204: 265–272.
17. Brown DA, London E (1998) Functions of lipid rafts in biological membranes. *Annu Rev Cell Dev Biol* 14:111–136.
18. Carroll AM, Zalutsky MR, Benacerraf B, Greene MI (1984) Monoclonal antibodies to tissue-associated antigens as antitumor reagents. *Surv Synth Pathol Res* 3:189–200.
19. Hubert RS, et al. (1999) STEAP: a prostate-specific cell-surface antigen highly expressed in human prostate tumors. *Proc Natl Acad Sci USA* 96:14523–14528.
20. Abe A, et al. (1992) Improved inhibitors of glucosylceramide synthase. *J Biochem* 111: 191–196.
21. Hakomori S (2003) Structure, organization, and function of glycosphingolipids in membrane. *Curr Opin Hematol* 10:16–24.
22. Nudelman ED, et al. (1988) A novel tumor-associated, developmentally regulated glycolipid antigen defined by monoclonal antibody ACFH-18. *J Biol Chem* 263: 13942–13951.
23. Hakomori S (1984) Tumor-associated carbohydrate antigens. *Annu Rev Immunol* 2: 103–126.
24. Hellström I, Brankovan V, Hellström KE (1985) Strong antitumor activities of IgG3 antibodies to a human melanoma-associated ganglioside. *Proc Natl Acad Sci USA* 82: 1499–1502.
25. Durrant LG, Harding SJ, Green NH, Buckberry LD, Parsons T (2006) A new anticancer glycolipid monoclonal antibody, SC104, which directly induces tumor cell apoptosis. *Cancer Res* 66:5901–5909.
26. Bremer EG, et al. (1984) Characterization of a glycosphingolipid antigen defined by the monoclonal antibody MBr1 expressed in normal and neoplastic epithelial cells of human mammary gland. *J Biol Chem* 259:14773–14777.
27. Mabry M, Speak JA, Griffin JD, Stahel RA, Bernal SD (1985) Use of SM-1 monoclonal antibody and human complement in selective killing of small cell carcinoma of the lung. *J Clin Invest* 75:1690–1695.
28. Cheung NK, et al. (1985) Monoclonal antibodies to a glycolipid antigen on human neuroblastoma cells. *Cancer Res* 45:2642–2649.
29. Welt S, Carswell EA, Vogel CW, Oettgen HF, Old LJ (1987) Immune and nonimmune effector functions of IgG3 mouse monoclonal antibody R24 detecting the disialoganglioside GD3 on the surface of melanoma cells. *Clin Immunol Immunopathol* 45:214–229.
30. Okada Y, Mugnai G, Bremer EG, Hakomori S (1984) Glycosphingolipids in detergent-insoluble substrate attachment matrix (DISAM) prepared from substrate attachment material (SAM). Their possible role in regulating cell adhesion. *Exp Cell Res* 155: 448–456.
31. Hughes-Jones NC, Gorick BD, Howard JC (1983) The mechanism of synergistic complement-mediated lysis of rat red cells by monoclonal IgG antibodies. *Eur J Immunol* 13:635–641.
32. Nichols B (2003) Caveosomes and endocytosis of lipid rafts. *J Cell Sci* 116:4707–4714.
33. Sillence DJ (2007) New insights into glycosphingolipid functions—storage, lipid rafts, and translocators. *Int Rev Cytol* 262:151–189.
34. Riemann D, et al. (2001) Caveolae/lipid rafts in fibroblast-like synoviocytes: ectopeptidase-rich membrane microdomains. *Biochem J* 354:47–55.
35. Dalskov SM, et al. (2005) Lipid raft localization of GABA A receptor and Na+, K+-ATPase in discrete microdomain clusters in rat cerebellar granule cells. *Neurochem Int* 46:489–499.
36. Bourrguignon LY, et al. (1995) Involvement of CD44 and its variant isoforms in membrane-cytoskeleton interaction, cell adhesion and tumor metastasis. *J Neurooncol* 26:201–208.
37. Allen JA, Halverson-Tamboli RA, Rasenick MM (2007) Lipid raft microdomains and neurotransmitter signalling. *Nat Rev Neurosci* 8:128–140.
38. Carlsson L, Ronquist G, Eliasson R, Egberg N, Larsson A (2006) Flow cytometric technique for determination of prostasomal quantity, size and expression of CD10, CD13, CD26 and CD59 in human seminal plasma. *Int J Androl* 29:331–338.
39. Utleg AG, et al. (2003) Proteomic analysis of human prostasomes. *Prostate* 56: 150–161.
40. Masuda K, et al. (2006) AHNP-streptavidin: a tetrameric bacterially produced antibody surrogate fusion protein against p185her2/neu. *Oncogene* 25:7740–7746.
41. Svennerholm L, Fredman P (1980) A procedure for the quantitative isolation of brain gangliosides. *Biochim Biophys Acta* 617:97–109.
42. Xia MQ, Tone M, Packman L, Hale G, Waldmann H (1991) Characterization of the CAMPATH-1 (CDw52) antigen: biochemical analysis and cDNA cloning reveal an unusually small peptide backbone. *Eur J Immunol* 21:1677–1684.